High-power single-polarization and single-transverse-mode fiber laser with an all-fiber cavity and fiber-grating stabilized spectrum

Chi-Hung Liu and Almantas Galvanauskas

Department of Electrical Engineering and Computer Science, University of Michigan, 1301 Beal Avenue, Ann Arbor, Michigan 48109-2122

Victor Khitrov, Bryce Samson, Upendra Manyam, Kanishka Tankala, and David Machewirth

Nufern, 7 Airport Park Road, East Granby, Connecticut 06026

Stefan Heinemann

Fraunhofer USA, Center for Laser Technology, 46025 Port Street, Plymouth, Michigan 48170

Received August 5, 2005; revised manuscript received September 17, 2005; accepted September 21, 2005

Conventionally, large-mode-area (LMA) fiber lasers use free-space polarizing components to achieve linear polarization output. External components, however, significantly limit laser robustness and power scalability. We demonstrate, to the best of our knowledge, the first high-power all-fiber cavity single-polarization single-transverse-mode LMA fiber laser, without the use of free-space polarizing components. This has been achieved by using tightly coiled high-birefringence 20 μm core LMA fiber. The lasing spectrum at 1085 nm has been stabilized by a fiber grating, spliced at one end of a LMA fiber. Up to 405 W of single-polarization output with a polarization extinction of >19 dB with a narrow spectrum (1.9 nm FWHM) and in a single-transverse mode ($M^2 < 1.1$) has been demonstrated. The simplicity of a monolithic-cavity approach is highly beneficial for a number of applications, including the use of a fiber laser for nonlinear wavelength conversion and for coherent and spectral beam combining. © 2006 Optical Society of America

OCIS codes: 060.2320, 060.2280.

The rapid development of high-power large-mode-area (LMA) fibers has led to recent demonstrations of 1–2 kW fiber lasers producing single-transverse-mode output beams.[1,2] This achievement is particularly important due to the highly practical aspects of fiber laser technology, such as compatibility with monolithic designs, high efficiency, and high reliability. Furthermore, fiber geometry appears to be ideally suited for further power scaling by employing coherent and spectral beam combining methods,[3,4] which potentially can lead to $\geqslant 10$ kW power high beam quality fiber lasers. One important technical challenge on this power scaling path is that beam combining critically requires single-polarization output fiber lasers. So far, however, such single-polarization LMA fiber lasers have been either based on the use of free-space polarizing components[5,6] or are complex master-oscillator–power-amplifier (MOPA) setups with in-line polarizing and isolating components.[7] Limitations imposed by such approaches are multifold. The use of bulk components is unsuitable for monolithic all-fiber designs, a significant practical impediment. Both free-space and in-line polarization components at present have limited power handling capacity, thus limiting the power scalability of single-polarization fiber lasers. Here we demonstrate a monolithic-cavity single-polarization cw LMA fiber laser with output powers exceeding 400 W in a single transverse mode and a spectrally stabilized narrow-linewidth output beam. This approach is unique in its simplicity: unlike other demonstrated high-power PM fiber laser designs, it does not use any free-space or in-line polarizing components or highly specialized single-polarization fibers.[8] Additionally, we demonstrate that 20 μm LMA core fiber monolithic cavities can include other spliced-in fiber components, such as narrow-linewidth fiber Bragg gratings (FBGs) for stabilization of the laser spectrum. The absence of polarizing components significantly facilitates the power scalability of this approach. This simple and robust all-fiber design is particularly attractive for beam combining as well as for a broad variety of other applications where single-polarization output is critical, such as nonlinear wavelength conversion using second-harmonic generation (SHG) or optical parametric oscillation (OPO).

Single-transverse and single-polarization mode operation in a highly birefringent LMA fiber can be achieved by exploiting two processes. First, higher-order modes can be suppressed by using conventional fiber-bending-induced differential loss between fundamental and higher-order modes in low-NA LMA-core fibers.[9] Second, stress-induced birefringence significantly increases the effective refractive index of one of the fundamental-mode polarizations, thus enabling one to achieve bending-induced loss differentiation between different LP_{01} mode polarizations as well. As shown in Ref. 10, the refractive index for the light polarized parallel to the stress direction (i.e., polarized along the x axis in the fiber cross section picture in Fig. 1) is significantly increased by the photoelastic effect, while for the polarization perpendicular

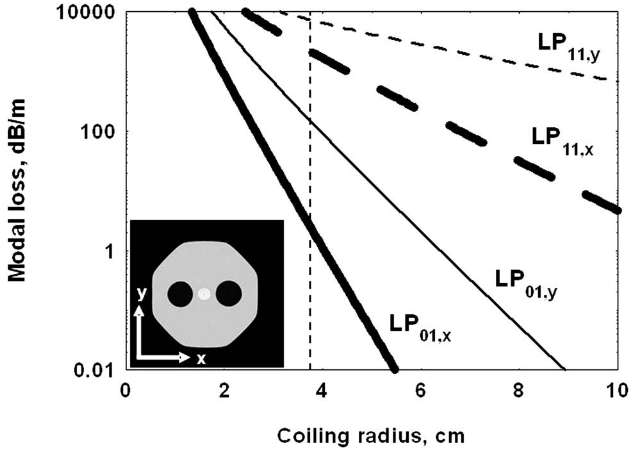

Fig. 1. Calculated bending loss for eigenpolarized spatial modes of 20 μm and 0.06 NA core highly birefringent ($\Delta n = 3\times 10^{-4}$) LMA fiber. A picture of fiber cross section with principal axes is also shown.

to the stress direction (i.e., polarized along the y axis) the refractive index remains nearly unchanged. In general, a lower effective refractive index corresponds to a weaker guidance of the correspondingly polarized mode and consequently to a higher susceptibility to the bending. Therefore with a properly selected core refractive index and fiber-bending radius the x-polarized LP_{01} mode can remain impervious to the bending, while higher-order modes and the y-polarized LP_{01} mode can experience large bending-induced loss. Calculated transverse- and polarization-mode bending-loss characteristics for 20 μm 0.06-NA core highly birefringent ($\Delta n = 3 \times 10^{-4}$) LMA fiber used in this work are shown in Fig. 1. In the experiment fiber was coiled to 7.5 cm in diameter (marked by the vertical dashed line), at which the calculated bending loss of >1 dB/m is relatively high. However, negligible reduction of the slope efficiency observed experimentally at this coiling radius indicates that the model overestimates bending-induced loss, and a tighter coiling than predicted needs to be used.

The setup of the fiber laser is shown in Fig. 2. An Yb-doped, panda-type, highly birefringent LMA double-clad fiber, whose cross section is shown in the inset of Fig. 1, is used as the gain medium in the system. The fiber has a 20 μm core and 400 μm octagon-shaped pump cladding with 0.06 and 0.45 NA for the core and the cladding, respectively. The fiber length of 33 m has been selected to optimize pump absorption at 940 nm. One end of the Yb-doped fiber was straight cleaved and the other end was spliced with a high reflectivity ($R > 99\%$) fiber Bragg grating at 1085 nm imprinted into an identical 20 μm core and 0.06 NA LMA fiber. The splicing procedure was carefully developed to produce negligible loss and inter-modal scattering at the splice (<0.1 dB). A picture of the splice is also shown in Fig. 2. The laser cavity was formed by a straight cleaved end (3.5% Fresnel reflection) and the high-reflectivity FBG. The free fiber end on the grating side was angle cleaved with $\sim 11°$ to eliminate end reflections. The Yb-doped fiber was coiled with 7.5 cm diameter, which allowed us to achieve single polarization in a single-transverse mode at the output. Three fiber-coupled pump modules operating at 915, 940, and 976 nm wavelengths were wavelength multiplexed and coupled from the straight-cleaved end. One more pump module operating at 915 nm was coupled from the angle cleaved end with a FBG. All four pump modules provided a maximum of 610 W of pump power coupled into the fiber. Fiber was heat sunk through a conductive heat-removal arrangement, which is much more efficient than convective heat removal in air and which was sufficient to eliminate thermal effects in the fiber at all used pump powers.

Figure 3 shows the measured output power of the laser. With the total 610 W of coupled pump power, up to 405 W of the laser output has been achieved with the slope efficiency of 65.9%. Minor slope-efficiency reduction compared with that for an uncoiled fiber (70.9%) indicates a minor effect of the coiling-induced extra loss of the "slow" x-polarized LP_{01} mode. The inset in Fig. 3 shows 1085.2 nm centered laser spectra at 184 and 405 W, revealing spectral broadening from 1.2 to 1.9 nm with increasing output power. This broadening indicates the reduction of threshold due to the increase of gain in the Yb fiber, which directly relates to and increases monotonically with pump power. We found that, compared with the spectral width of the fiber grating (~ 1.5 nm), the laser spectral width is still well confined by the grating, which implies the possibility of narrowing down the laser linewidth by using narrow spectral-width fiber gratings.

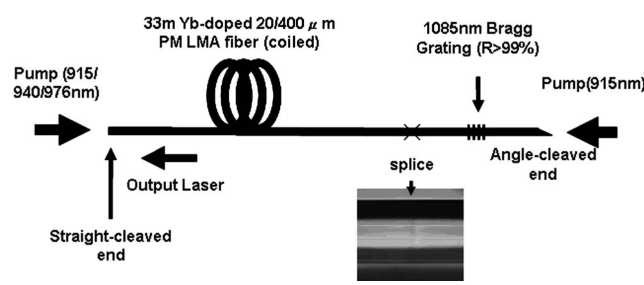

Fig. 2. Monolithic-cavity single-polarization LMA fiber laser.

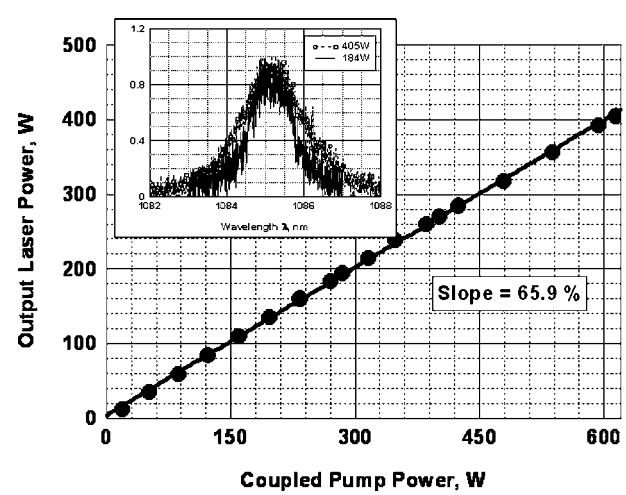

Fig. 3. Output laser power and spectrum.

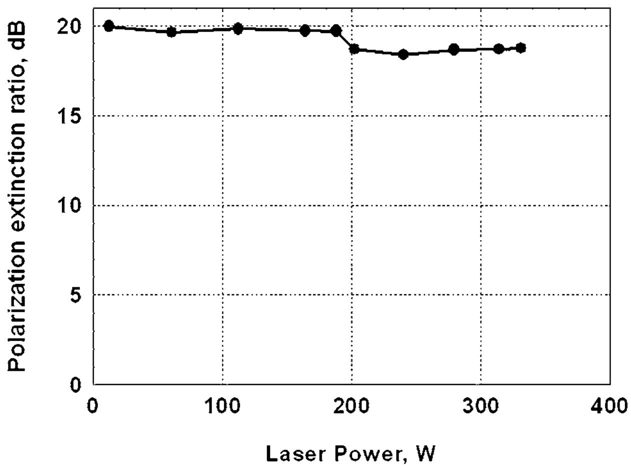

Fig. 4. Polarization extinction ratio at different laser output powers.

Figure 4 shows the polarization extinction ratio (PER) of the laser output measured at different laser powers. No significant power dependence has been observed. At all power levels measured the PER was >18.8 dB. Note, however, that at <200 W output the measured PER is ~20 dB with an ~1.2 dB drop at ~200 W. For output powers >200 W the PER power dependence remains flat. We identified this 1.2 dB drop to be caused solely by the change of measurement setup, which was necessary at higher powers, and not by any abrupt change in laser behavior itself. We have also measured output beam M^2 values at different output power levels. At all powers measured $M^2 < 1.1$, with an observed tendency to slightly increase with increasing output power (from $M^2 = 1.02$ at the threshold to $M^2 = 1.05$ at the highest power). This tendency is at least partly associated with the increasing difficulty of accurately measuring beam quality at higher beam powers due to an increasing scattered-light background.

A particular practical advantage of 20 μm core low-NA LMA fibers is that they are dual mode and, consequently, can be spliced together with negligible modal scattering loss. For comparison, 30 μm 0.06 NA core LMA fibers support five modes, making it practically very difficult to achieve low scattering in the splice between such fibers. Therefore our demonstrated 20 μm PM LMA fiber-based monolithic laser-cavity designs can be extended to include other fiber components, such as all-fiber signal–pump combiners[11] or additional fiber gratings. Systems using all-fiber pump combiners could be completely monolithic. The use of two fiber gratings as reflectors at both laser-cavity ends would bring two significant advantages: an increase in the stimulated Raman scattering (SRS) threshold, thus permitting a significant increase in the output power, and achieving narrow spectral bandwidths at high output powers. Indeed, according to our previous simulation for 20 μm core LMA fiber[12] two-grating laser cavity eliminates feedback at the Raman band and consequently can increase the SRS threshold to ~2 kW for a 30 m long laser cavity (to much higher powers for shorter laser cavities) with an assumed 45 dB residual reflection for angle cleaved fiber ends. One should note that SBS is not a real limiting factor in this configuration as long as the laser bandwidth is sufficiently broad to suppress Brillouin gain. Our estimates indicate that $\Delta\lambda \sim 0.1$ nm is sufficient to achieve this, thus permitting further significant linewidth reduction compared with our current result.

In summary, we have demonstrated a simple technique to achieve high-power single-polarization and single-transverse mode operation from a monolithic LMA-fiber laser cavity. The practical significance of such a laser is that it does not use any free-space or in-line polarizing or isolating components and can be built by using standard off-the-shelf Yb-doped double-clad fibers. The achieved 405 W output was limited by the available pump power. Our analysis indicates that multi-kW output powers should be achievable with this approach. Measured >18.8 dB polarization extinction did not degrade with output power. Also, it is likely that the obtained PER value is measurement limited and higher values are practically achievable. A particular feature of the demonstrated laser is its narrow-linewidth operation, achieved by including a narrow-linewidth fiber grating into the monolithic laser cavity. Such monolithic PM and narrow-linewidth design are particularly valuable for future fiber laser power scaling using both coherent and spectral beam combining techniques, and the whole class of other applications—for example, high power nonlinear wavelength conversion.

C.-H. Liu's e-mail address is liuch@umich.edu; V. Khitrov's e-mail address is vkhitrov@nufern.com.

References

1. Y. Jeong, J. K. Sahu, D. N. Payne, and J. Nilsson, Opt. Express **12**, 6088 (2004).
2. V. P. Gapontsev, D. V. Gapontsev, N. S. Platonov, O. Shkurikhin, V. Fomin, A. Mashkin, M. Abramov, and S. Ferin, in *The European Conference on Lasers and Electro-Optics*, paper CJ1-1.
3. J. Anderegg, S. J. Brosnan, M. E. Weber, H. Komine, and M. G. Wickham, in Proc. SPIE **4974**, 1 (2003).
4. S. J. Augst, A. K. Goyal, R. L. Aggarwal, T. Y. Fan, and A. Sanchez, Opt. Lett. **28**, 331 (2003).
5. C.-H. Liu, A. Galvanauskas, and B. Ehlers, in *Proceedings of Advanced Solid-State Photonics*, (2004), MA5.
6. A. Liem, J. Limpert, T. Schreiber, M. Reich, H. Zellmer, A. Tunnermann, A. Carter, and K. Tankala, in *European Conference on Lasers and Electro-Optics* (Optical Society of America, 2004), paper CMS4.
7. Y. Jeong, J. Nilsson, J. K. Sahu, D. B. Soh, P. Dupriez, C. A. Codemard, S. Baek, D. N. Payne, R. Horley, J. A. Alvarez-Chavez, and P. W. Turner, Opt. Lett. **30**, 955 (2005).
8. D. A. Nolan, G. E. Berkey, M.-J. Li, X. Chen, W. A. Wood, and L. A. Zenteno, Opt. Lett. **29**, 1855 (2004).
9. J. P. Koplow, D. A. V. Kliner, and L. Goldberg, Opt. Lett. **25**, 442 (2000).
10. K. Okamoto, Appl. Opt. **23**, 2638 (1984).
11. F. Gonthier, L. Martineau, N. Azami, M. Faucher, F. Séguin, D. Stryckman, and A. Villeneuve, in Proc. SPIE **5535**, 266 (2004).
12. C.-H. Liu, B. Ehlers, F. Doerfel, S. Heinemann, A. Carter, K. Tankala, J. Farroni, and A. Galvanauskas, Electron. Lett. **40**, 1471 (2004).